Spectroscopy and electronic structure of jet-cooled NiCu

Zhenwen Fu and Michael D. Morse
Department of Chemistry, University of Utah, Salt Lake City, Utah 84112

(Received 7 September 1988; accepted 9 December 1988)

Diatomic nickel–copper, NiCu, has been investigated by resonant two-photon ionization spectroscopy in a jet-cooled molecular beam. Six band systems have been identified over the range 11 500–16 500 cm^{-1}. The ground state of NiCu has been determined to be $X\,^2\Delta_{5/2}$, with $\omega_e'' = 273.01 \pm 1.15$ cm^{-1}, $\omega_e''x_e'' = 1.00 \pm 0.38$ cm^{-1}, and $r_e'' = 2.233 \pm 0.006$ Å. This state derives from a strongly bound (2.05 ± 0.10 eV) $3d^{10}_{Cu}3d^{9}_{Ni}4s\sigma^2$ configuration. Excited states observed in this work derive from the more weakly bound $3d^{10}_{Cu}3d^{8}_{Ni}4s\sigma^24s\sigma^{*1}$ configuration, and are characterized by smaller vibrational frequencies (191–208 cm^{-1}) and a longer bond length (2.351 ± 0.005 Å) than the ground $X\,^2\Delta_{5/2}$ state.

I. INTRODUCTION

The electronic structure and chemical bonding of small transition metal clusters are topics of considerable current interest from both the experimental[1–4] and theoretical[5–8] points of view. In addition to providing information about the small clusters themselves, investigations of these topics provide important data which is relevant to many branches of chemistry and physics, ranging from heterogeneous catalysis and surface chemistry to solid-state physics. In all of these fields, an understanding of the chemical bonding which occurs between metals is important. By investigating diatomic and triatomic metals in spectroscopic detail, the nature of the metal–metal chemical bond may be ascertained, even for complicated systems such as the transition metals.

Gas-phase spectroscopic investigations of transition metal dimers and trimers have thus far concentrated on the more easily prepared homonuclear species such as V_2,[9] Cr_2,[10–13] Fe_2,[14] Co_2,[14] Ni_2,[15] Cu_2,[16] Mo_2,[17–20] Ag_2,[16] Re_2,[21] Pt_2,[22] Au_2,[16] Ni_3,[23] Cu_3,[24–26] and Ag_3.[27] Among the mixed transition metal species only CuAg,[28,29] CuAu,[30] and CrMo[31] have yet been spectroscopically studied in the gas phase. This pattern of study has occurred in part because the laser vaporization technique has only been in general use for a few years, and investigators have usually chosen to concentrate their efforts on the simpler single-component species. In addition, however, a general method of conveniently generating mixed clusters has not existed. In a few cases mixed clusters have been produced by laser vaporization of a target alloy,[32–36] and recently mixed clusters have been generated by vaporization of one metal in the presence of a volatile organometallic compound of a second metal.[37] The former method is limited by the availability of the target alloy. The latter method relies on the facile photodissociation of the organometallic compound during the laser vaporization of the target metal, and may be compromised if the ejected ligands reattach to the metal during supersonic expansion. Moreover, this method is limited by the availability of suitable volatile organometallic compounds. In this paper we report a more general method for the production of mixed metal clusters, in which powdered metals are mixed and then compacted into a solid, vaporizable disk under high pressure. The disk can be made with nearly any mixture of metal powders, and in any ratio. Using this method of sample preparation we anticipate that most of the mixed transition metal dimers can be systematically investigated. As has been demonstrated by a number of electron spin resonance (ESR) studies of matrix-isolated mixed transition metal clusters,[38–42] chemical bonding in the mixed dimers is at least as intriguing as the bonding in the homonuclear systems. In addition to the possibilities of single or multiple bonds, and high or low spin, mixed transition metal dimers include the possibility of partial charge transfer from one atom to the other, resulting in molecules with nonzero dipole moments. Such effects may well be important in bimetallic catalysts, or in conventional heterogeneous catalysts with alkali atoms added as promoting agents.

In this paper we present the first spectroscopic investigation of a jet-cooled mixed transition metal dimer, NiCu. We have chosen this species for study in part because it is the simplest of the open *d*-shell transition metal dimers: it lacks only one electron of having a closed *d*-shell. As such, NiCu should possess a relatively sparse set of excited electronic states, and it should be possible to make a detailed assignment of these states, correlating the potential energy curves out to the separated atom limit. As experimentalists, an important role is to provide detailed data for a few benchmark molecular systems, which will become the proving grounds for improved theoretical methods. The likelihood of succeeding in a detailed analysis of the spectra of NiCu makes this molecule particularly promising for such a role.

In the present investigation resonant two-photon ionization spectroscopy has been applied to the NiCu molecule, resulting in the observation of six electronic band systems between 11 500 and 16 500 cm^{-1}. These are assigned as transitions between the ground electronic configuration of $3d^{10}_{Cu}3d^{9}_{Ni}4s\sigma^2$ [correlating to the Ni $3d^94s^1(^3D)$ + Cu $3d^{10}4s^1(^2S)$ separated atom limit] and an excited electronic configuration of $3d^{10}_{Cu}3d^{8}_{Ni}4s\sigma^24s\sigma^{*1}$, which correlates to Ni $3d^84s^2(^3F)$ + Cu $3d^{10}4s^1(^2S)$ separated atoms. One of the band systems has been rotationally resolved, allowing the ground state to be identified as $^2\Delta_{5/2}$, arising from the $3d^{10}_{Cu}3d^{9}_{Ni}4s\sigma^2$ electronic configuration. This is in agreement with the one available theoretical calculation.[43]

In Sec. II we present a brief description of our experimental apparatus and methods. Vibronic and rotationally resolved spectra of NiCu are presented in Sec. III, along with

 0021-9606/89/073417-10$02.10

excited state lifetime measurements. These results are then interpreted in Sec. IV, where the electronic structure of NiCu is discussed in some detail. Finally, Sec. V closes the paper with a summary of our findings.

II. EXPERIMENTAL

The molecular beam apparatus employed in these investigations of NiCu is essentially identical to that used in previous studies of Al_3,[44] Pt_2,[22] and C_3[45] in this laboratory. The metal cluster source uses an arrangement very similar to that of O'Brien *et al.*,[46] in which the second harmonic of a Q-switched Nd:YAG laser is focused onto a rotating metal disk located in the throat of a pulsed supersonic expansion of helium. Following expansion into vacuum, the molecular beam is skimmed and admitted into the ionization region of a reflectron time-of-flight mass spectrometer. Resonant two-photon ionization spectroscopic studies are then performed by directing a pulsed dye laser down the molecular beam axis, and crossing this with the output of a pulsed excimer laser operating on ArF (193 nm, 6.42 eV). The mass spectrum is then digitized at a rate of 100 MHz, and the experimental cycle is repeated at a rate of 10 Hz, with data collection under computer control.

The key experimental advance which made the present work possible was the development of a technique for production of mixed metal disks suitable for laser vaporization. As we began this work, we became aware of Knight's success[47] in generating CP radicals by laser vaporization of a mixture of carbon and red phosphorus, which had been compacted under high pressure. Accordingly, an equimolar mix of copper (2.5–3.0 μ, Alfa) and nickel ($< 63\,\mu$, EM Science) powders was prepared in a glove box under argon, and transferred to a high-pressure mold assembly. This consisted of two opposable mild steel pistons with polished faces, which snugly fit into an aluminum collar which could be disassembled after use. The use of different metals for the pistons and the collar was found to greatly reduce the tendency of the press to seize when subjected to high pressure. The mixed metal powders were then pressed under 50 000 psi using a hydraulic press, the mold assembly was disassembled, and the solid mixed metal disk was stored under argon until it could be used. Failure to store the disk under argon resulted in the formation of metal oxides, which severely reduced the NiCu signal.

Freshly prepared NiCu disks were reddish and metallic in color, though not as red as copper. Since nickel–copper alloy is silver in color, the compacted metal powders clearly do not form an alloy, but consist of microscopic domains of copper and nickel. Moreover, NiCu disks could be easily resurfaced on the lathe, with the removed material falling off as a fine dust. This again indicated that no alloy formation had occurred when the powders were pressed. However, NiCu disks that had been subjected to the intense radiation used to vaporize the metals displayed silver tracks on their surface, demonstrating that local alloying was taking place under the laser vaporization conditions.

Once the mixed NiCu disks had been made, mixed Ni–Cu clusters were generated as easily as the single-component clusters. Figure 1 displays a mass spectrum of the metal

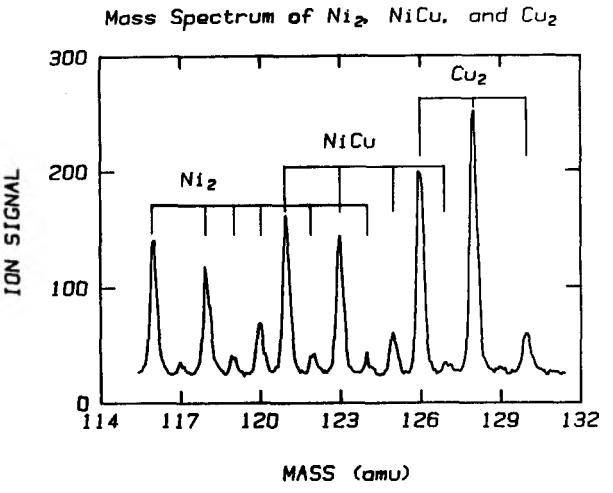

FIG. 1. Mass spectrum of Ni_2, NiCu, and Cu_2, obtained with ArF radiation (6.42 eV, 192 nm). In this experiment an equimolar mix of nickel and copper was vaporized, resulting in the formation of all three diatomic metals.

dimers produced with this source, obtained using ArF radiation (6.42 eV, 192 nm) as the ionization laser. The NiCu mixed diatomics of mass 121, 123, and 125 amu were monitored independently as the dye laser was scanned, allowing direct recording of the spectra of the isotopically selected dimers. In all of the spectra reported here a dye laser (Molectron, model DL-II) pumped by the second harmonic of a Q-switched Nd:YAG laser (Quantel, model 581-C) was used to excite the NiCu molecule, and the excited state was then ionized by ArF radiation (6.42 eV, 192 nm) (Questek, model 2420). High-resolution studies were carried out using an intracavity etalon and accessories (Molectron, DL 224), which was pressure scanned from 0 to 1 atm using SF_6. Lifetimes of the excited states were measured by time-delayed resonant two-photon ionization methods.

III. RESULTS

A. Vibronic spectra of NiCu

Figure 2 displays a low-resolution resonant two-photon ionization spectrum of $^{58}Ni^{63}Cu$ over the range 11 300–14 500 cm^{-1} (885–690 nm). This spectrum was obtained using the laser dyes LDS 698, 750, 751, 821, and 867 and their mixtures, and is a composite of several scans. Further scans to the blue to 16 500 cm^{-1} (606 nm) were also carefully performed using rhodamine 640, DCM, and LDS 698, but no additional transitions were observed. Although no attempt has been made to scale the intensity of spectroscopic transitions by normalizing to the intensity of the dye laser, the intensities of the features in Fig. 2 are meaningful since the dye laser fluence (~ 10 mJ/cm^2) did not vary strongly over the broad range of the LDS dyes, and the low intensity gaps between dyes were overcome by the use of mixtures.

Six band systems have been identified in Fig. 2, where they are labeled as systems A–F. Although only the cold bands are labeled, hot bands corresponding to $v'' = 1$ have been found for all of the band systems, and hot bands with $v'' = 2$ have been found for system B. Altogether, 76 vibronic bands have been identified as belonging to the six band systems A–F, thereby accounting for nearly all of the

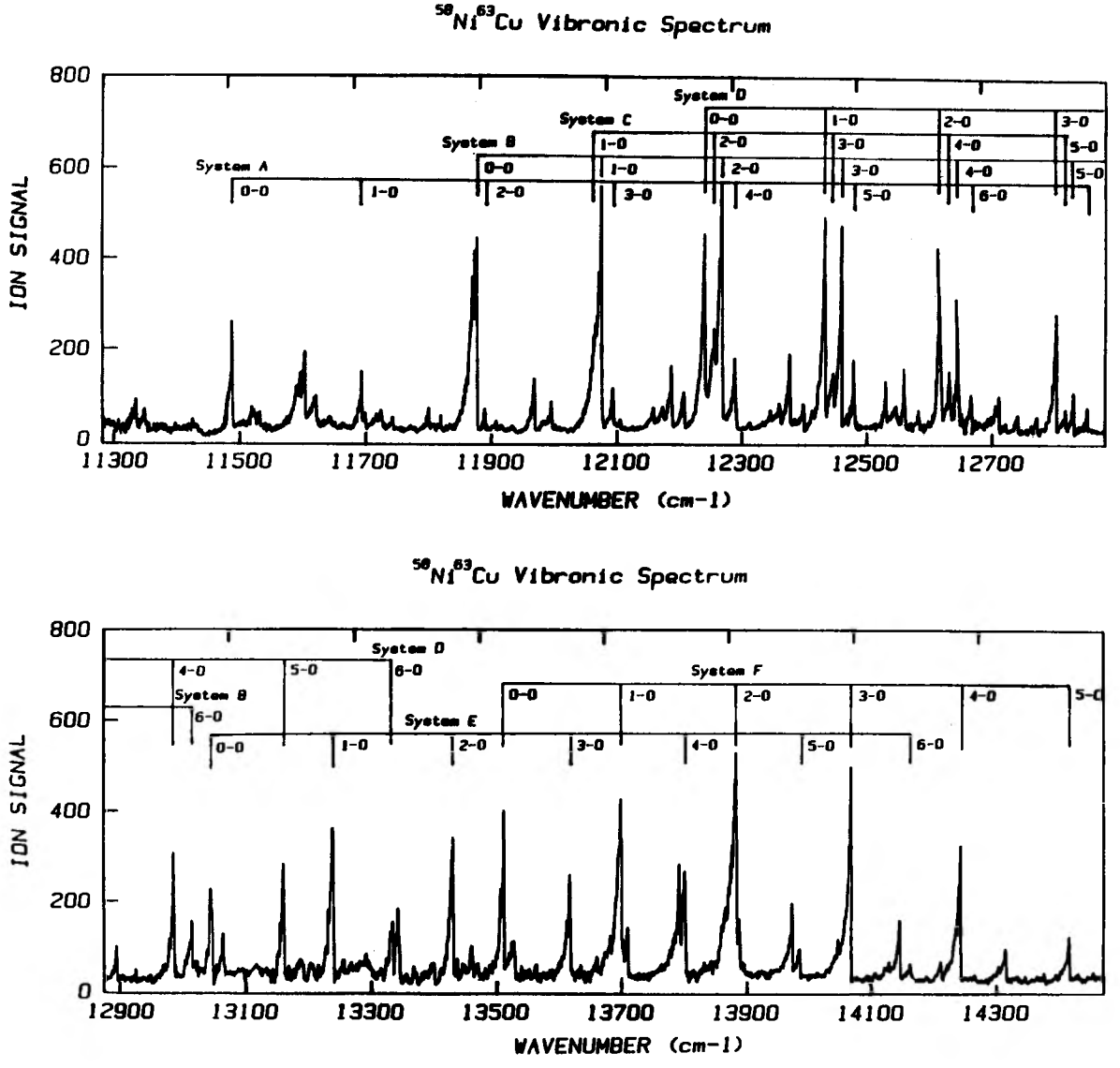

FIG. 2. Low-resolution spectrum of NiCu, obtained by resonant two-photon ionization spectroscopy with a scanning dye laser followed by photoionization with ArF radiation. The cold bands of systems A–F are marked. Unmarked features are nearly all accounted for as hot bands derived from these systems. See Table I for hot band assignments.

features in the spectrum. Band assignments were based on the intensities of the bands and on the isotope shifts between the NiCu species of mass 121 ($^{58}Ni^{63}Cu$), mass 123 ($^{58}Ni^{65}Cu$ and $^{60}Ni^{63}Cu$), and mass 125 ($^{60}Ni^{65}Cu$). The bandhead positions and assignments, along with isotope shifts and least-squares fitted band positions are given in Table I for all 76 bands of $^{58}Ni^{63}Cu$.

Least-square fits of the band positions for each band system have been performed to extract ω_e' and $\omega_e'x_e'$ for each of the excited electronic states. In addition, the least-squares fit of systems A, C, D, E, and F has enabled $\Delta G_{1/2}''$ to be extracted, while the observation of $v''=2$ hot bands in system B has allowed the vibrational frequency, ω_e'', and anharmonicity, $\omega_e''x_e''$, of the ground state to be determined. These spectroscopic constants, along with the band origins, ν_{00}, of each band system are reported in Table II. The $\Delta G_{1/2}''$ values listed in Table II for each band system are all consistent within experimental error, giving $\Delta G_{1/2}''=271.7\pm0.5$ cm^{-1}. This value is much larger than the vibrational frequencies of any of the upper states, which range from $\omega_e'=191.68\pm0.85$ cm^{-1} to $\omega_e'=207.75\pm0.71$ cm^{-1}. The chemical bonding in ground state NiCu is clearly much stronger than in any excited states observed here.

Lifetimes of selected bands were measured by time-delayed resonant two-photon ionization methods; the resulting $1/e$ decay times are given in Table I. All of the excited states are quite long lived, with lifetimes ranging from 3 to 9 μs. If the only decay process is fluorescence to the ground electronic state, such lifetimes correspond to absorption oscillator strengths ranging from 9×10^{-4} to 2×10^{-3}. As discussed in Sec. IV, however, other low-lying electronic states exist, and fluorescence to these states is also possible. Therefore the true oscillator strengths of the observed band systems are probably below 1×10^{-3}. This is too small for the observed transitions to be fully allowed, but is certainly larger than expected for spin-forbidden transitions. (For com-

TABLE I. Vibronic bands of $^{58}Ni^{63}Cu$.

System	Band	Observed frequency[a] (cm^{-1})	Fitted frequency[b] (cm^{-1})	Difference (cm^{-1})	Isotope shift Mass 123[c] (cm^{-1})	Isotope shift Mass 125[c] (cm^{-1})	Lifetime[d] (μs)
A	0–0	11 485.46	11 485.35	0.11	0.00	0.00	
	1–0	11 690.96	11 689.93	1.03	− 2.29	− 3.82	
	2–0	11 889.82	11 891.35	− 1.53	...	...	
	3–0	12 090.35	12 089.60	0.75	− 3.93	− 8.49	8.16 ± 1.66
	4–0	12 285.39	12 284.69	0.70	− 5.68	− 11.96	8.90 ± 0.99
	5–0	12 477.60	12 476.61	0.99	− 7.61	− 14.80	
	6–0	12 664.42	12 665.37	− 0.95	− 7.94	− 16.32	
	7–0	12 849.84	12 850.97	− 1.13	− 9.10	− 19.16	
	2–1	11 619.82	11 619.66	0.16	− 0.37	− 1.49	
	3–1	11 815.91	11 817.91	− 2.00	− 1.59	− 3.46	
	5–1	12 204.97	12 204.92	0.05	− 4.91	− 8.19	8.52 ± 1.54
	6–1	12 395.20	12 393.68	1.52	− 5.92	− 12.27	8.57 ± 0.70
	7–1	12 601.82	12 601.79	0.03	− 6.96	...	
B	0–0	11 872.85	11 872.25	0.60	0.20	0.39	
	1–0	12 070.11	12 069.88	0.23	− 1.60	− 3.00	4.34 ± 0.24
	2–0	12 263.78	12 264.28	− 0.50	− 3.33	− 6.66	4.39 ± 0.44
	3–0	12 456.02	12 455.43	0.59	− 5.50	− 10.20	4.66 ± 0.85
	4–0	12 643.70	12 643.35	0.35	− 6.17	− 12.79	5.03 ± 0.50
	5–0	12 828.07	12 828.02	0.05	− 7.73	− 15.46	
	6–0	13 008.15	13 009.46	− 1.31	− 8.58	...	
	0–1	11 601.74	11 601.24	0.50	2.19	4.65	
	1–1	11 797.60	11 798.87	− 1.27	0.57	1.91	
	2–1	11 992.11	11 993.27	− 1.16	− 1.20	− 2.21	
	3–1	12 184.69	12 184.42	0.27	− 3.75	− 5.83	6.07 ± 0.50
	4–1	12 373.26	12 372.34	0.92	− 4.99	− 9.99	5.12 ± 0.30
	5–1	12 557.71	12 557.02	0.69	− 5.29	− 11.91	7.14 ± 0.29
	6–1	12 738.51	12 738.46	0.05	...	...	
	0–2	11 331.85	11 332.23	− 0.38	4.21	...	
	1–2	11 530.71	11 529.86	0.85	0.96	...	
	2–2	11 723.95	11 724.26	− 0.31	− 0.77	...	
	4–2	12 102.71	12 103.33	− 0.62	− 3.94	...	
	6–2	12 469.91	12 469.45	0.46	...	...	
C	2–0	12 252.75	12 252.81	− 0.06	− 2.55	− 5.44	4.41 ± 1.08
	3–0	12 443.34	12 442.93	0.41	− 5.49	...	
	4–0	12 630.23	12 630.38	− 0.15	− 6.29	...	
	5–0	12 814.97	12 815.17	− 0.20	...	...	
	3–1	12 171.04	12 171.26	− 0.22	− 2.01	− 4.63	
	4–1	12 358.67	12 358.71	− 0.04	− 3.99	− 9.42	
	5–1	12 543.75	12 543.49	0.26	− 5.51	...	
D	0–0	12 236.21	12 236.56	− 0.35	0.41	0.0	5.82 ± 0.47
	1–0	12 428.96	12 427.81	1.51	− 1.69	− 2.12	5.54 ± 0.54
	2–0	12 615.91	12 615.38	0.53	− 2.65	− 5.29	
	3–0	12 799.87	12 799.29	0.58	− 4.09	− 8.64	6.77 ± 0.80
	4–0	12 979.09	12 979.52	− 0.43	− 5.24	− 10.96	7.23 ± 0.50
	5–0	13 154.92	13 156.08	− 1.17	− 5.25	− 12.87	6.23 ± 0.75
	6–0	13 328.66	13 328.98	− 0.32	− 8.01	− 16.39	7.15 ± 0.59
	0–1	11 965.51	11 965.19	0.32	1.40	4.40	
	1–1	12 155.48	12 156.44	− 0.96	1.30	...	
	2–1	12 342.86	12 344.02	− 1.16	− 0.62	...	
	3–1	12 528.16	12 527.92	0.24	− 2.65	− 3.97	
	4–1	12 708.52	12 708.16	0.36	− 3.53	− 7.06	7.49 ± 0.49
	5–1	12 885.36	12 884.72	0.64	− 4.55	− 9.55	6.33 ± 0.39
	6–1	13 058.19	13 057.61	0.58	− 5.24	...	
E	0–0	13 038.03	13 039.92	− 1.89	0.41	0.40	
	1–0	13 232.77	13 233.01	− 0.25	− 1.43	− 2.38	3.62 ± 0.37
	2–0	13 423.24	13 423.37	− 0.13	− 2.61	− 6.06	2.69 ± 0.49
	3–0	13 611.71	13 610.99	0.72	− 4.60	− 8.73	3.97 ± 0.25
	4–0	13 795.70	13 795.87	− 0.17	− 6.39	− 12.26	
	5–0	13 979.52	13 978.01	1.51	− 6.57	− 13.35	
	6–0	14 157.62	14 157.42	0.20	− 8.03	− 16.81	
	0–1	12 769.91	12 767.70	2.21	2.20	5.10	
	2–1	13 150.63	13 151.15	− 0.52	...	...	
	3–1	13 338.58	13 338.76	− 0.18	− 0.17	− 2.64	5.04 ± 0.36
	4–1	13 523.73	13 523.64	0.08	− 2.83	− 6.69	
	5–1	13 704.70	13 705.79	− 1.09	− 4.38	− 8.91	
	6–1	13 884.69	13 885.20	− 0.51	− 5.70	...	

TABLE I (*continued*).

System	Band	Observed frequency[a] (cm^{-1})	Fitted frequency[b] (cm^{-1})	Difference (cm^{-1})	Isotope shift Mass 123[c] (cm^{-1})	Isotope shift Mass 125[c] (cm^{-1})	Lifetime[d] (μs)
F	0–0	13 505.46	13 504.96	0.50	0.00	0.00	
	1–0	13 692.77	13 693.15	−0.38	−1.23	−2.33	
	2–0	13 876.99	13 877.84	−0.85	−2.61	−5.63	4.70 ± 0.24
	3–0	14 060.72	14 059.05	1.67	−4.48	−8.71	5.12 ± 0.37
	4–0	14 235.81	14 236.76	−0.96	−5.25	−10.96	5.44 ± 0.40
	5–0	14 411.00	14 410.99	0.01	−7.17	−13.22	5.95 ± 0.89
	3–1	13 785.64	13 786.94	−1.30	−1.80	−5.66	5.16 ± 0.28
	4–1	13 965.86	13 964.66	1.21	−3.25	−6.09	5.58 ± 0.53
	5–1	14 139.54	14 138.88	0.66	−5.35	−9.95	6.01 ± 0.49
	6–1	14 309.05	14 309.62	−0.57	−6.33	−11.17	

[a] Frequency observed for $^{58}Ni^{63}Cu$. Relative uncertainty in the band positions is estimated as $\pm 2\ cm^{-1}$, but the absolute band positions may be in error by as much as $10\ cm^{-1}$.

[b] Band positions were fitted to the equation $\nu = \nu_{00} + \omega_e' v' - \omega_e' x_e' (v'^2 + v') - \Delta G_{1/2}''$ for $v'' = 0,1$ and $\nu = \nu_{00} + \omega_e' v' - \omega_e' x_e' (v'^2 + v') - \omega_e'' v'' + \omega_e'' x_e'' (v''^2 + v'')$ for $v'' = 0, 1, 2$. The resulting values of the parameters ν_{00}, ω_e', $\omega_e' x_e'$, ω_e'', $\omega_e'' x_e''$, and $\Delta G_{1/2}''$ are given in Table II.

[c] Isotope shifts are measured at the bandheads, with the convention that a negative shift indicates that the designated isotopic band lies to the red of the $^{58}Ni^{63}Cu$ band.

[d] The quoted errors are $\pm 1\ \sigma$, as determined from a least-squares fit.

parison, the $a\ ^3\Sigma_u^+ \leftarrow X\ ^1\Sigma_g^+$ transition in matrix-isolated Cu_2 exhibits an oscillator strength of $f = 3 \times 10^{-7}$, based on the $a\ ^3\Sigma_u^+$ lifetime of 27 ms.)[48] The low oscillator strength of the observed transitions will be considered in more detail in Sec. IV, where a comprehensive description of the electronic structure of NiCu is provided.

B. Rotationally resolved spectra of $^{58}Ni^{63}Cu$

Figure 3 displays high resolution ($0.05\ cm^{-1}$) scans of the 1–0 (7303 Å) and 3–0 (7112 Å) bands of system F, along with simulated spectra. As is also evident in Fig. 2, both bands are red degraded, with the R branch forming a sharp and intense bandhead. A series of P branch lines are observed going off to the red, and a weak Q branch is observed which quickly decreases in intensity with increasing J. This distribution in spectral intensity among the P, Q, and R branches, with strong P and R branches and a Q branch which rapidly diminishes with increasing J, is characteristic of bands with $\Delta\Lambda = 0$ [or $\Delta\Omega = 0$ in Hund's case (a) or (c)].[49]

In atomic nickel the $3d^9 4s^1$, ^3D and $3d^8 4s^2$, ^3F terms lie lowest in energy, with only $240\ cm^{-1}$ separating the J-averaged term energies.[50] In forming the chemical bond with copper, $3d^{10} 4s^1$, ^2S the strongest bond will clearly be formed with the nickel atom in its $3d^9 4s^1$, ^3D term, resulting in a molecular configuration of $3d^{10}_{Cu}\, 3d^9_{Ni}\, (4s\sigma)^2$. Such a configuration lacks one electron of being a closed shell configura-

TABLE II. Spectroscopic constants of $^{58}Ni^{63}Cu$.[a]

State	ν_{00}[b–d]	ω_e[b]	$\omega_e x_e$[b]	B_e	α_e	r_e (Å)
$F\ \Omega = 5/2$	13 504.96 ± 1.04	191.68 ± 0.85	1.75 ± 0.12	0.101 08 ± 0.000 12[e]	0.001 04 ± 0.000 06[e]	2.3513 ± 0.005[f]
E	13 039.93 ± 0.83	195.83 ± 0.67	1.37 ± 0.09			
D	12 236.56 ± 0.56	194.92 ± 0.46	1.84 ± 0.06			
C[d]	11 864.57 ± 1.72	198.12 ± 1.15	1.33 ± 0.14			
B	11 872.25 ± 0.49	200.87 ± 0.38	1.62 ± 0.05			
A[d]	11 485.35 ± 1.02	207.75 ± 0.71	1.58 ± 0.08			
$X\ ^2\Delta_{5/2}$	···	273.01 ± 1.15	1.00 ± 0.38	0.112 08 ± 0.000 18[e,g]	0.000 55 ± 0.000 16[e,g]	2.2330 ± 0.006[f]

[a] All constants reported in this table are given in wave numbers (cm^{-1}), except r_e, which is given in Angstroms (Å).

[b] Vibronic bands were fitted to the formula $\nu = \nu_{00} + \omega_e' v' - \omega_e' x_e' (v'^2 + v') - \Delta G_{1/2}'' v''$ for systems in which only $v'' = 0,1$ were observed. For the B–X band system $v'' = 0$, 1, and 2 were observed, and the band positions were fitted to the formula $\nu = \nu_{00} + \omega_e' v' - \omega_e' x_e' (v'^2 + v') - \omega_e'' v'' + \omega_e'' x_e'' (v''^2 + v'')$. From this fit the ground state parameters ω_e'' and $\omega_e'' x_e''$ were obtained, and were found to be consistent with the values of $\Delta G_{1/2}''$ found in the other fits. The quoted uncertainty is $\pm 1\sigma$, as determined from the least-squares fit.

[c] Owing to the uncertainty in absolute calibration of the dye laser used in this work, the uncertainty in ν_{00} is estimated as $\pm 10\ cm^{-1}$ for all band systems. The relative uncertainty between band system origins is much smaller, estimated at $\pm 2\ cm^{-1}$.

[d] As discussed in the text, it is likely that some of the observed band systems originate from electronically excited molecules, probably from the $\Omega = 3/2$ excited spin–orbit component of the $X\ ^2\Delta$ state. Based on band intensities, systems A and C may arise from this or other metastable electronic states.

[e] Uncertainty is given as $\pm 1\sigma$, as obtained in the least-squares fit, and does not include the estimated $\pm 0.15\%$ error expected in the calibration of the 0.2196 cm^{-1} etalon. A more conservative estimate would triple the errors listed above.

[f] Uncertainty in bond length is reported as $\pm 3\sigma$, thereby including the uncertainty in calibration of the monitoring etalon.

[g] B_e and α_e are derived for the $X\ ^2\Delta_{5/2}$ state from the measured B_0 assuming the validity of the Pekeris relationship (Ref. 51).

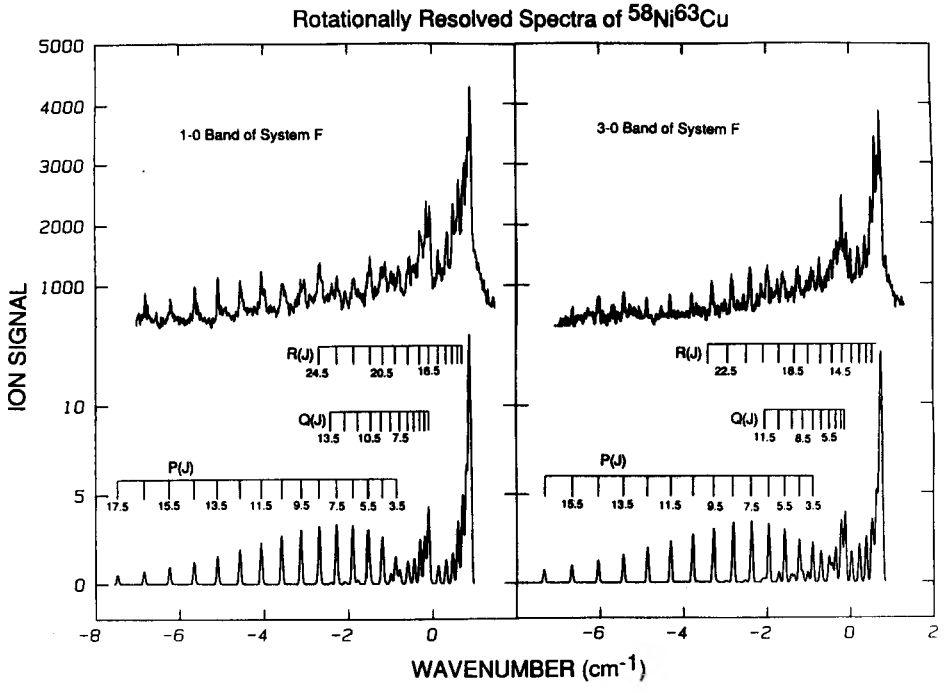

FIG. 3. High-resolution spectra of the 1–0 and 3–0 bands of system F of $^{58}Ni^{63}Cu$. Observed spectra are shown in the upper portion of the figure, while simulated spectra are shown below. The band origins, ν_0, are located at 0 cm^{-1}, and the frequency axis is measured relative to this position. Line positions are given in Table III. Simulated spectra are calculated using the rotational constants from footnote c of Table III, along with a laser linewidth of 0.05 cm^{-1}, and an assumed rotational temperature of 15 K.

tion, and the hole can be in either a $d\sigma$, $d\pi$, or $d\delta$ orbital, localized on the nickel atom. Thus the NiCu ground state is expected to be $^2\Sigma^+_{1/2}$, $^2\Pi_{1/2}$, $^2\Pi_{3/2}$, $^2\Delta_{3/2}$, or $^2\Delta_{5/2}$. Based on these considerations and the observations described in the preceding paragraph we have considered $\Omega' = 5/2 \leftarrow \Omega'' = 5/2$, $\Omega' = 3/2 \leftarrow \Omega'' = 3/2$, and $\Omega' = 1/2 \leftarrow \Omega'' = 1/2$ transitions in our analysis of the high resolution spectra. A careful examination of all possible assignments consistent with these values of Ω' and Ω'' has permitted the unambiguous assignment of system F as an $\Omega' = 5/2 \leftarrow {}^2\Delta_{5/2}$ transition. The observed and fitted line positions of both the 1–0 and 3–0 bands are given in Table III. The rotational and derived constants of $^{58}Ni^{63}Cu$ are provided in Table II.

IV. DISCUSSION

With the spectroscopic data described in Sec. III in hand, it is now possible to make some progress in understanding the electronic structure of NiCu. Table IV lists the term manifold of NiCu, as determined for the lowest states of the separated atoms. In setting up the correlation between the separated atom and molecular states we have assumed that the $3d$ electrons make no direct contribution to the chemical bonding in NiCu. This assumption is justified by the small orbital radius, $\langle r \rangle$, of the $3d$ electrons, which is calculated by numerical Hartree–Fock methods to be 0.511 and 0.486 Å for nickel and copper, respectively.[52] These orbital radii are so much smaller than the measured internuclear distances listed in Table II that $3d$ contributions to the chemical bonding are negligible. Experimentally, $3d$ contributions to the chemical bonding may be excluded on the basis of the near equality of the bond lengths (r_e), bond strengths (D_0), and vibrational frequencies (ω_e) of Ni_2, NiCu, and Cu_2. These properties are compared in Table V, where less than 4% variation is found among the three molecules considered.

The strongly bound states (bond order of 1) of NiCu all derive from the $3d^9 4s^1(^3D)$ Ni + $3d^{10}4s^1(^2S)$ Cu separated atom limit, with the two $4s$ electrons spin pairing to form a σ bond. This results in $^2\Sigma^+$, $^2\Pi$, and $^2\Delta$ states, of which the $^2\Delta_{5/2}$ component is shown by the present study to be the ground state. In the upper states of all six band systems, the vibrational frequency is within 9 of 200 cm^{-1}, which represents a reduction to 73% of the ground state value. This corresponds to a reduction of the harmonic force constant to 54% of the ground state value. On this basis the upper states may be thought of as possessing a bond order of 1/2.

In principle, a bond order of 1/2 could be achieved by either promoting a nonbonding $3d$ electron to the $4s\sigma^*$ antibonding orbital, or by removing a $4s\sigma$ bonding electron and placing it in the $3d^9_{Ni}$ core, forming a $3d^{10}_{Cu}3d^{10}_{Ni}4s\sigma^1$ configuration. The latter possibility leads only to a $^2\Sigma^+_{1/2}$ term, which would not be optically accessible from the $^2\Delta_{5/2}$ ground state.[54] Moreover, it would correlate to the $3d^{10}4s^0(^1S)$ Ni + $3d^{10}4s^1(^2S)$ Cu separated atom asymptote, which lies 13 997.4 cm^{-1} above the lowest separated atom state. On this basis we may safely conclude that the upper states observed in this work have the molecular electronic configuration $3d^{10}_{Cu}3d^8_{Ni}4s\sigma^2 4s\sigma^{*1}$, which derives from the $3d^8 4s^2(^3F)$ Ni + $3d^{10}4s^1(^2S)$ Cu separated atom limit.

In the separated atom limit, the observed transitions correspond to the $3d^8 4s^2(^3F) \leftarrow 3d^9 4s^1(^3D)$ transition of atomic nickel. This transition is rigorously forbidden under electric dipole selection rules, since it is a $g \leftarrow g$ transition. When the NiCu molecule is formed, however, the center of inversion is removed, and this transition gains some slight intensity. The low oscillator strength of our observed transitions therefore arises from the forbidden nature of the transition in the separated atoms.

Candidates for the upper states observed in this study are the $^2\Sigma^+_{1/2}$, $^2\Pi_{1/2}$, $^2\Pi_{3/2}$, $^2\Delta_{3/2}$, $^2\Delta_{5/2}$, $^2\Phi_{5/2}$, and $^2\Phi_{7/2}$

TABLE III. Observed and fitted line positions for the F band system of $^{58}Ni^{63}Cu$.[a]

	1–0 band				3–0 band			
Assignment	Observed line position[b]	Fitted line position[c]	Residual	Comment	Observed line position[b]	Fitted line position[c]	Residual	Comment
$R(2.5)$	0.595	0.589	0.006		···	0.557	···	
$R(3.5)$	0.698	0.702	−0.004		···	0.652	···	
$R(4.5)$	0.803	0.790	0.013		···	0.718	···	R-branch head
$R(5.5)$	0.866	0.853	0.013		···	0.755	···	R-branch head
$R(6.5)$	···	0.892	···	R-branch head	···	0.764	···	R-branch head
$R(7.5)$	···	0.906	···	R-branch head	···	0.745	···	R-branch head
$R(8.5)$	···	0.896	···	R-branch head	···	0.696	···	
$R(9.5)$	0.866	0.861	0.005		···	0.619	···	
$R(10.5)$	0.803	0.801	0.002		···	0.514	···	
$R(11.5)$	0.709	0.717	−0.008		0.357	0.380	−0.023	
$R(12.5)$	0.593	0.608	−0.015		0.200	0.217	−0.017	
$R(13.5)$	0.481	0.474	0.007		0.041	0.026	0.015	
$R(14.5)$	0.314	0.316	−0.002		−0.187	−0.194	0.007	
$R(15.5)$	0.123	0.133	−0.010		−0.444	−0.443	−0.001	
$R(16.5)$	−0.088	−0.075	−0.013	Blended with $Q(2.5)$	−0.724	−0.720	−0.004	
$R(17.5)$	−0.301	−0.307	0.006		···	−1.026	···	
$R(18.5)$	−0.577	−0.564	−0.013		···	−1.360	···	
$R(19.5)$	−0.817	−0.846	0.029	Blended with $Q(7.5)$	−1.723	−1.723	0.000	
$R(20.5)$	−1.153	−1.152	−0.001		−2.115	−2.115	0.000	
$R(21.5)$	···	−1.483	···	Blended with $Q(10.5)$	−2.532	−2.535	0.003	
$Q(2.5)$	−0.084	−0.108	0.024	Blended with $R(16.5)$	−0.095	−0.125	0.030	
$Q(3.5)$	−0.175	−0.194	0.019		−0.212	−0.225	0.013	
$Q(4.5)$	−0.320	−0.305	−0.015		···	−0.354	···	
$Q(5.5)$	−0.468	−0.441	−0.027		···	−0.512	···	
$Q(6.5)$	−0.603	−0.601	−0.002		···	−0.698	···	
$Q(7.5)$	−0.817	−0.786	−0.031	Blended with $R(19.5)$	···	−0.912	···	
$Q(8.5)$	−1.002	−0.995	−0.007		···	−1.155	···	
$Q(9.5)$	···	−1.229	···		···	−1.427	···	
$Q(10.5)$	···	−1.488	···	Blended with $R(21.5)$	···	−1.728	···	
$Q(11.5)$	···	−1.772	···		···	−2.057	···	
$Q(12.5)$	−2.089	−2.080	−0.009		···	−2.414	···	
$P(3.5)$	−0.874	−0.891	0.017		···	−0.908	···	
$P(4.5)$	−1.203	−1.201	−0.002		−1.232	−1.231	−0.001	
$P(5.5)$	−1.514	−1.536	0.022		−1.586	−1.584	−0.002	
$P(6.5)$	−1.896	−1.895	−0.001		−1.975	−1.964	−0.011	
$P(7.5)$	−2.286	−2.279	−0.007		−2.377	−2.374	−0.003	
$P(8.5)$	−2.691	−2.687	−0.004		−2.819	−2.812	−0.007	
$P(9.5)$	−3.128	−3.121	−0.007		−3.285	−3.279	−0.006	
$P(10.5)$	−3.568	−3.578	0.010		−3.779	−3.774	−0.005	
$P(11.5)$	−4.073	−4.061	−0.012		−4.297	−4.298	0.001	
$P(12.5)$	−4.559	−4.568	0.009		−4.856	−4.851	−0.005	
$P(13.5)$	−5.109	−5.100	−0.009		−5.446	−5.432	−0.014	
$P(14.5)$	−5.651	−5.656	0.005		−6.033	−6.042	0.009	
$P(15.5)$	−6.231	−6.237	0.006		−6.664	−6.680	0.016	
$P(16.5)$	−6.842	−6.843	0.001		···		···	

[a] All numerical values are in wave numbers (cm^{-1}).

[b] The observed line positions were measured by interpolating between the fringes of a 0.2196 cm^{-1} etalon. After fitting the line positions, a constant has been added to all observed and fitted line positions so that the band origin, ν_0, falls at 0.000 cm^{-1}.

[c] Fitted line positions are obtained by a least-squares fit of the observed line positions for each individual band to the formula $\nu = \nu_0 + B'J'(J'+1) - B''J''(J''+1)$. From the fit of the 1–0 band we obtain $\nu_0 = 0.000 \pm 0.0029$ cm^{-1}, $B'_1 = 0.099\,53 \pm 0.000\,10$ cm^{-1}, $B''_0 = 0.111\,86 \pm 0.000\,11$ cm^{-1}, while the fit of the 3–0 band provides $\nu_0 = 0.0000 \pm 0.0040$ cm^{-1}, $B'_3 = 0.097\,46 \pm 0.000\,12$ cm^{-1}, and $B''_0 = 0.111\,76 \pm 0.000\,13$ cm^{-1}. The small uncertainties in these parameters, small residuals in the fit, and agreement between the two independent fits of B''_0 support the assignment given.

states which arise from the $3d^{10}_{Cu}\,3d^{8}_{Ni}\,4s\sigma^2 4s\sigma^{*1}$ configuration of NiCu, and which correlate to the $3d^8 4s^2(^3F)$ Ni + $3d^{10}4s^1(^2S)$ Cu separated atom limit. We exclude the quartet ($S = 3/2$) states arising from this limit from consideration, on the assumption that intercombination transitions will be much weaker than our observed transitions, with much longer lifetimes. Of the doublet terms listed above, only $^2\Pi_{3/2}$, $^2\Delta_{3/2}$, $^2\Delta_{5/2}$, $^2\Phi_{5/2}$, and $^2\Phi_{7/2}$ are optically accessible from the ground $^2\Delta_{5/2}$ state of NiCu. Thus, five band systems should be observed in this study, yet we have identified six band systems in the observed spectra. There are only two possible explanations for the presence of a sixth band system in our data. Either, (1) it is an intercombination, with the upper state belonging to one of the components of the $^4\Sigma^-$, $^4\Pi$, $^4\Delta$, and $^4\Phi$ multiplets, or (2) it is an electronic hot band, in which the lower state of the transition is

TABLE IV. Term mainfold of low-lying states of NiCu.[a]

Separated atoms			Molecular NiCu		
Energy[b] (cm^{-1})	Atomic states Ni	Atomic states Cu	Molecular terms	Molecular configuration	Bond order[c]
0.00	$3d^9 4s^1(^3D)$	$3d^{10}4s^1(^2S)$	$^2\Sigma^+_{1/2}$, $^2\Pi_{1/2}$, $^2\Pi_{3/2}$, $^2\Delta_{3/2}$, $^2\Delta_{5/2}$,	$3d^{10}_{Cu}\,3d^{9}_{Ni}\,4s\sigma^2$	1
			$^4\Sigma^+_{1/2}$, $^4\Sigma^+_{3/2}$, $^4\Pi_{-1/2}$, $^4\Pi_{1/2}$, $^4\Pi_{3/2}$,	$3d^{10}_{Cu}\,3d^{9}_{Ni}\,4s\sigma^1 4s\sigma^{*1}$	0
			$^4\Pi_{5/2}$, $^4\Delta_{1/2}$, $^4\Delta_{3/2}$, $^4\Delta_{5/2}$, $^4\Delta_{7/2}$	$3d^{10}_{Cu}\,3d^{9}_{Ni}\,4s\sigma^1 4s\sigma^{*1}$	0
240.34	$3d^8 4s^2(^3F)$	$3d^{10}4s^1(^2S)$	$^2\Sigma^-_{1/2}$, $^2\Pi_{1/2}$, $^2\Pi_{3/2}$, $^2\Delta_{3/2}$, $^2\Delta_{5/2}$, $^2\Phi_{5/2}$, $^2\Phi_{7/2}$	$3d^{10}_{Cu}\,3d^{8}_{Ni}\,4s\sigma^2 4s\sigma^{*1}$	1/2
			$^4\Sigma^-_{1/2}$, $^4\Sigma^-_{3/2}$, $^4\Pi_{-1/2}$, $^4\Pi_{1/2}$, $^4\Pi_{3/2}$, $^4\Pi_{5/2}$,	$3d^{10}_{Cu}\,3d^{8}_{Ni}\,4s\sigma^2 4s\sigma^{*1}$	1/2
			$^4\Delta_{1/2}$, $^4\Delta_{3/2}$, $^4\Delta_{5/2}$, $^4\Delta_{7/2}$, $^4\Phi_{3/2}$, $^4\Phi_{5/2}$	$3d^{10}_{Cu}\,3d^{8}_{Ni}\,4s\sigma^2 4s\sigma^{*1}$	1/2
			$^4\Phi_{7/2}$, $^4\Phi_{9/2}$	$3d^{10}_{Cu}\,3d^{8}_{Ni}\,4s\sigma^2 4s\sigma^{*1}$	1/2
2678.48	$3d^9 4s^1(^1D)$	$3d^{10}4s^1(^2S)$	$^2\Sigma^+_{1/2}$, $^2\Pi_{1/2}$, $^2\Pi_{3/2}$, $^2\Delta_{3/2}$, $^2\Delta_{5/2}$	$3d^{10}_{Cu}\,3d^{9}_{Ni}\,4s\sigma^1 4s\sigma^{*1}$	0

[a] This table includes all separated atom limits below 12 000 cm^{-1} in energy.
[b] Separated atom energies are given by the weighted average over the atomic levels, using the energy levels of Ref. 50.
[c] Calculated assuming no d–d bonding contributions.

not the $^2\Delta_{5/2}$ ground state, but is electronically excited. In the latter case, the $^2\Delta_{3/2}$ state is the most likely possibility.

Based on the comparable band intensities and similar lifetimes of the six observed band systems, it is unlikely that one band system is an intercombination system, while all of the others preserve the value of S in the transition. Therefore we conclude that one (or more) of the observed band systems arises from an electronically excited lower state, probably the $^2\Delta_{3/2}$ state. Of the band systems shown in Fig. 2, systems A and C are noticeably less intense than the remaining band systems, and therefore may be electronic hot bands, originating from the $^2\Delta_{3/2}$ state. Proof or disproof of this conjecture must await further experimental work, however. In particular, high-resolution studies and stimulated emission probing of the lower states should greatly clarify the manifold of doublet states in NiCu.

This work should be compared to the one available theoretical investigation of NiCu by Shim.[43] In her study of NiCu, Shim calculated the doublet states arising from $3d^9 4s^1(^3D)$ Ni and $3d^{10}4s^1(^2S)$ Cu, using Hartree–Fock methods followed by configuration interaction allowing full reorganization within the $3d$ and $4s$ shells. The $^2\Delta$ state was found to lie lowest in energy at all levels of theory; when spin–orbit interactions were included, the $^2\Delta_{5/2}$ component was found to be the ground state. This is in agreement with the experimental results presented here. However, Shim calculates a bond length of 2.41 Å for the $X\,^2\Delta_{5/2}$ state of NiCu, nearly 0.2 Å longer than that measured in the present investigation. The calculated vibrational frequency of 347 cm^{-1} is considerably larger than that measured here. Finally, the calculated bond strength of 1.54 eV is too small by about 0.5 eV, indicating that a higher level of theory, probably including the $4p$ orbitals, is required.

The only other experimental work on NiCu prior to this study consists of a mass spectrometric measurement of the high-temperature gas-phase equilibrium

$$NiCu + Cu \rightleftarrows Cu_2 + Ni$$

by Kant, Strauss, and Lin.[53] In this investigation, a second-law value of $D_0(NiCu) = 2.06 \pm 0.22$ eV was obtained, while the third-law value was calculated to be $D_0(NiCu) = 2.14 \pm 0.25$ eV. A re-evaluation of their data by the third-law method, using the bond length and vibrational frequency obtained here for the ground $^2\Delta_{5/2}$ state, assuming electronic excitation energies to the $^2\Delta_{3/2}$, $^2\Pi_{3/2}$, $^2\Pi_{1/2}$, and $^2\Sigma_{1/2}$ states as calculated by Shim,[45] and using $D_0(Cu_2) = 2.01 \pm 0.08$ eV,[2] yields $D_0(NiCu) = 2.05 \pm 0.10$ eV, in excellent agreement with the second-law value. This is also in close agreement with $D_0(Cu_2)$ and $D_0(Ni_2)$, as shown in Table V, demonstrating the similarities in chemical bonding among this series of compounds.

V. CONCLUSIONS

The NiCu diatomic molecule has been investigated by resonant two-photon ionization spectroscopy in a jet-cooled molecular beam, and six band systems have been identified

TABLE V. Comparison of Ni_2, NiCu, and Cu_2.

Property	$^{58}Ni_2$	$^{58}Ni^{63}Cu$	$^{63}Cu_2$
r_e	2.200 ± 0.007 Å[a,b]	2.233 ± 0.006 Å[c]	2.2197 Å[e]
D_0	2.068 ± 0.01 eV[a]	2.05 ± 0.10 eV[d]	2.01 ± 0.08 eV[e]
ω_e	···	273.01 ± 1.15 cm^{-1}[c]	264.55 cm^{-1}[e]

[a] Reference 15.
[b] This value is r_0, not r_e.
[c] This work.
[d] Reference 53, reevaluated as described in Sec. IV.
[e] Reference 2.

over the frequency range 11 500–16 500 cm^{-1}. With the exception of one or two band systems which arise from electronically excited NiCu, these systems correspond to excitations from the $X\,^2\Delta_{5/2}$ ground state, which is characterized by $\omega_e'' = 273.01 \pm 1.15$ cm^{-1}, $\omega_e''x_e'' = 1.00 \pm 0.38$ cm^{-1}, and $r_e'' = 2.233 \pm 0.006$ Å.

The upper states are all more weakly bound, with ω_e' ranging from 192 to 208 cm^{-1}. One band system has been rotationally resolved, allowing the identification of the ground state as $X\,^2\Delta_{5/2}$, and establishing the bond length of the ground state. The upper state of this band system is characterized by $\Omega' = 5/2$, $r_e' = 2.351 \pm 0.005$ Å, $\omega_e' = 191.68 \pm 0.85$ cm^{-1}, and $\omega_e'x_e' = 1.75 \pm 0.12$ cm^{-1}. All spectroscopic constants are reported for the $^{58}Ni^{63}Cu$ isotopic modification.

The ground $X\,^2\Delta_{5/2}$ state of NiCu arises from the molecular configuration $3d\,^{10}_{Cu}\,3d\,^{9}_{Ni}\,4s\sigma^2$, which in turn correlates to $3d\,^9 4s^1(^3D)Ni + 3d\,^{10}4s^1(^2S)Cu$ separated atoms. Other states correlating to this limit are $^2\Delta_{3/2}$, $^2\Pi_{3/2}$, $^2\Pi_{1/2}$, and $^2\Sigma_{1/2}$, which are all expected to be strongly bound, along with a number of quartet ($S = 3/2$) states which are expected to be repulsive. Use of our spectroscopic parameters for the $X\,^2\Delta_{5/2}$ state, along with the estimated excitation energies to the other strongly bound states[43] has permitted a reevaluation of the bond strength of NiCu by the third-law method,[53] resulting in $D_0(NiCu) = 2.05 \pm 0.10$ eV. This is nearly identical with the bond strengths $D_0(Ni_2) = 2.068 \pm 0.01$ eV[15] and $D_0(Cu_2) = 2.01 \pm 0.08$ eV.[2]

The upper states derive from the $3d\,^8 4s^2(^3F)Ni + 3d\,^{10}4s^1(^2S)Cu$ separated atom limit, which is nearly degenerate with the $3d\,^9 4s^1(^3D)Ni + 3d\,^{10}4s^1(^2S)Cu$ separated atom limit. These states possess a molecular configuration of $3d\,^{10}_{Cu}\,3d\,^{8}_{Ni}\,4s\sigma^2 4s\sigma^{*1}$, which leads to a bond order of 1/2, accounting for the reduced value of ω_e' for these systems and for the observed increase in bond length.

Further work is in progress to clarify the molecular terms associated with each band system, and attempts will be made to locate the remaining strongly bound states of NiCu. At that time a complete picture of the electronic structure of this simplest open-*d* shell transition metal dimer should be available.

ACKNOWLEDGMENTS

We are grateful to Professor William H. Breckenridge for the use of the intracavity etalon employed in the high resolution studies. We also gratefully acknowledge research support from the National Science Foundation under Grant No. CHE-85-21050. Acknowledgment is also made to the Donors of the Petroleum Research Fund, administered by the American Chemical Society, for partial support of this research.

[1]W. Weltner, Jr. and R. J. Van Zee, Annu. Rev. Phys. Chem. **35**, 291 (1984).
[2]M. D. Morse, Chem. Rev. **86**, 1049 (1986).
[3]A. Kaldor, D. M. Cox, and M. R. Zakin, Adv. Chem. Phys. **70**, 211 (1988).
[4]D. J. Trevor and A. Kaldor, in *High Energy Processes in Organometallic Chemistry*, edited by K. S. Suslick [ACS Symp. Ser. **333**, 43 (1987)].
[5]J. Koutecky and P. Fantucci, Chem. Rev. **86**, 539 (1986).
[6]D. R. Salahub, in *Ab Initio Methods in Quantum Chemistry-II*, edited by K. P. Lawley [Adv. Chem. Phys. **69**, 447 (1987)].
[7]I. Shim, Mat.-Fys. Meddr. Danske Vidensk. Selsk. (16 Res. Rep. of Niels Bohr Fellows) **41**, 147 (1985).
[8]S. R. Langhoff and C. W. Bauschlicher, Jr., Annu. Rev. Phys. Chem. **39**, 181 (1988).
[9]P. R. R. Langridge-Smith, M. D. Morse, G. P. Hansen, and R. E. Smalley, J. Chem. Phys. **80**, 593 (1984).
[10]Y. M. Efremov, A. N. Samoilova, and L. V. Gurvich, Opt. Spectrosc. **36**, 381 (1974).
[11]D. L. Michalopoulos, M. E. Geusic, S. G. Hansen, D. E. Powers, and R. E. Smalley, J. Phys. Chem. **86**, 3914 (1982).
[12]S. J. Riley, E. K. Parks, L. G. Pobo, and S. Wexler, J. Chem. Phys. **79**, 2577 (1983).
[13]V. E. Bondybey and J. H. English, Chem. Phys. Lett. **94**, 443 (1983).
[14]D. G. Leopold and W. C. Lineberger, J. Chem. Phys. **85**, 51 (1986).
[15]M. D. Morse, G. P. Hansen, P. R. R. Langridge-Smith, L.-S. Zheng, M. E. Geusic, D. L. Michalopoulos, and R. E. Smalley, J. Chem. Phys. **80**, 5400 (1984).
[16]Numerous studies; see Ref. 2 for details.
[17]K. H. Becker and M. Schürgers, Z. Naturforsch. Teil A **26**, 2072 (1971).
[18]Y. M. Efremov, A. N. Samoilova, V. B. Kozhukhovsky, and L. V. Gurvich, J. Mol. Spectrosc. **73**, 430 (1978).
[19]A. N. Samoilova, Y. M. Efremov, D. A. Zhuravlev, and L. V. Gurvich, Khim. Vys. Energ. **8**, 229 (1974).
[20]J. B. Hopkins, P. R. R. Langridge-Smith, M. D. Morse, and R. E. Smalley, J. Chem. Phys. **78**, 1627 (1983).
[21]D. G. Leopold, T. M. Miller, and W. C. Lineberger, J. Am. Chem. Soc. **108**, 178 (1986).
[22]S. Taylor, G. W. Lemire, Y. Hamrick, Z.-W. Fu, and M. D. Morse, J. Chem. Phys. **89**, 5517 (1988).
[23]J. R. Woodward, S. H. Cobb, and J. L. Gole, J. Phys. Chem. **92**, 1404 (1988).
[24]M. D. Morse, J. B. Hopkins, P. R. R. Langridge-Smith, and R. E. Smalley, J. Chem. Phys. **79**, 5316 (1983).
[25]W. H. Crumley, J. S. Hayden, and J. L. Gole, J. Chem. Phys. **84**, 5250 (1986).
[26]E. A. Rohlfing and J. J. Valentini, Chem. Phys. Lett. **126**, 113 (1986).
[27]M. A. Duncan (personal communication).
[28]J. Ruamps, Spectrochim. Acta. Suppl. **11**, 329 (1957).
[29]K. C. Joshi and K. Majumdar, Proc. Phys. Soc. London **78**, 197 (1961).
[30]J. Ruamps, C. R. Hebd. Seances Acad. Sci. **239**, 1200 (1954).
[31]Y. M. Efremov, A. N. Samoilova, and L. V. Gurvich, Chem. Phys. Lett. **44**, 108 (1976).
[32]V. E. Bondybey and J. H. English, J. Chem. Phys. **79**, 4746 (1983).
[33]V. E. Bondybey, G. P. Schwartz, and J. H. English, J. Chem. Phys. **78**, 11 (1983).
[34]R. G. Wheeler, K. LaiHing, W. L. Wilson, J. D. Allen, R. B. King, and M. A. Duncan, J. Am. Chem. Soc. **108**, 8101 (1986).
[35]Y. Liu, Q.-L. Zhang, F. K. Tittel, R. F. Curl, and R. E. Smalley, J. Chem. Phys. **85**, 7434 (1986).
[36]S. C. O'Brien, Y. Liu, Q.-L. Zhang, J. R. Heath, F. K. Tittel, R. F. Curl, and R. E. Smalley, J. Chem. Phys. **84**, 4074 (1986).
[37]K. LaiHing, P. Y. Cheng, and M. A. Duncan, J. Phys. Chem. **91**, 6521 (1987).
[38]R. J. Van Zee and W. Weltner, Jr., High Temp. Sci. **17**, 181 (1984).
[39]C. A. Baumann, R. J. Van Zee, and W. Weltner, Jr., J. Chem. Phys. **79**, 5272 (1983).
[40]C. A. Baumann, R. J. Van Zee, and W. Weltner, Jr., J. Phys. Chem. **88**, 1815 (1984).
[41]R. J. Van Zee and W. Weltner, Jr., Chem. Phys. Lett. **107**, 173 (1984).
[42]R. J. Van Zee and W. Weltner, Jr., Chem. Phys. Lett. **150**, 329 (1988).
[43]I. Shim, Theor. Chim. Acta. **54**, 113 (1980).
[44]Z.-W. Fu, G. W. Lemire, Y. Hamrick, S. Taylor, J.-C. Shui, and M. D. Morse, J. Chem. Phys. **88**, 3524 (1988).
[45]G. W. Lemire, Z.-W. Fu, Y. Hamrick, S. Taylor, and M. D. Morse, J. Phys. Chem. (in press).
[46]S. C. O'Brien, Y. Liu, Q. Zhang, J. R. Heath, F. K. Tittel, R. F. Curl, and R. E. Smalley, J. Chem. Phys. **84**, 4074 (1986).
[47]L. B. Knight, Jr., J. T. Petty, S. T. Cobranchi, D. Feller, and E. R. Davidson, J. Chem. Phys. **88**, 3441 (1988).
[48]V. E. Bondybey, J. Chem. Phys. **77**, 3771 (1982).

[49]G. Herzberg, *Molecular Spectra and Molecular Structure I. Spectra of Diatomic Molecules*, 2nd ed. (Van Nostrand Reinhold, New York, 1950), p. 207.
[50]C. E. Moore, Natl. Bur. Stand. Circ. 467 (1949, 1952).
[51]C. L. Pekeris, Phys. Rev. **45**, 98 (1934); see also Ref. 49, p. 108.
[52]C. Froese Fischer, *The Hartree–Fock Method for Atoms* (Wiley, New York, 1977), p. 39.
[53]A. Kant, B. Strauss, and S.-S. Lin, J. Chem. Phys. **52**, 2384 (1970).
[54]The analog of the $3d^{10}_{Cu}\,3d^{10}_{Ni}\,(4s\sigma)^1\,{}^2\Sigma^+$ state of NiCu, which is dismissed from further consideration here, is evidently the ground state of the isoelectronic ion, Cu_2^+. See A. D. Sappey, J. E. Harrington, and J. C. Weisshaar, J. Chem. Phys. **88**, 5243 (1988), and other work to be published.